Supplemental figure 1: Skeletal analysis of neonatal pups. (A) *Skax23*^{m1Jus} pups were smaller in size-smaller mutant pup is shown by white arrow next to 5 wildtype pups of normal size. (B) Whole-mount staining in newborn mice using Alcian blue for cartilage and Alizarin red for bone of WT (left) and mutant mice (right). (C) Compared to bones of WT (wild-type) mice, the length of humeri of *Skax23*^{m1Jus} mutant mice was decreased by 19% ± 10.00 (p = 0.0927, not statistically significant). Similarly, the length of femurs of *Skax23*^{m1Jus} mutant mice was reduced by 16% ± 5.188 (p = 0.0169), while the length of their tibia was shorter by 9% ± 5.276 (not statistically significant, p= 0.1301). Skulls of mutant mice were smaller anterior-posteriorly than in WT mice (20% ± 11.16, although not statistically significant, p= 0.1207). No significant difference in vertebrae was observed between *Skax23*^{m1Jus} mutant mice and WT controls.

Supplemental figure 2: Identification of the gene mutated in *Skax23*^{m1Jus} mutant mice. (A) Whole genome linkage scans identified a 41 Mb haplotype on chromosome 5 that was heterozygous in B6 in all 21 mice analyzed. The graph shows the percentage of heterozygous mice for the C57BL/6J allele for each SNP (n =149) for each chromosome. B. The table shows the genotypes of these same 21 mice at 13 SNPs selected from the candidate region on chromosome 5. (C) Fine mapping delineated the candidate region on chromosome 5 to an 11 Mb interval flanked by rs13478444 and rs13478483. Heterozygous genotypes at the C57BL/6J allele in panels B and C are shaded.

Supplemental figure 3: *Rpl5*+/- mice have ventricular septal defect but not craniofacial abnormality. Mice were euthanized and cardiac and craniofacial sections were generated for histology. (A) No newborn WT mice exhibited cardiac malformations (n=3), while 5/6 mutant mice displayed VSD and 1 mouse also had double outlet right ventricle (DORV; not shown). Analysis of 9 adult mice (WT n=2 and mutant n=7) showed no evidence of VSD by histology. Analysis of the newborn craniofacial structures by (B) micro-CT (WT n=1 and *Rpl5*+/- n=3) or (C) histology (WT n=1 and *Rpl5*+/- n=4) showed no evidence of cleft palate or other craniofacial abnormality.

Supplemental figure 4: E12.5 embryos. (A, B) Whole embryo images at E12.5 from 2 litters to

demonstrate embryo size and fetal liver color.

Supplemental figure 5: E14.5 embryos. (A, B) Whole embryo images at E14.5 from 2 litters to demonstrate embryo size and fetal liver color.

Supplemental figure 6: Analysis of terminal erythroid differentiation shows a severe defect in E12.5 fetal liver cells. Analysis of differentiation in E12.5 FL by CD44 vs. Ter119 flow cytometry staining showed a significant block in terminal red cell differentiation with a significant 3-fold increase in the proerythroblast (proEB) population in *Rpl5*+/- animals (A, B). This differentiation block has diminished by E14.5 with a 1.5-fold increase in this proerythroblast block in *Rpl5*+/- mice (C, D). E12.5 WT n=9, *Rpl5*+/- n=9 (3 litters); E14.5 WT n=9, *Rpl5*+/- n=12 (4 litters).

Supplemental figure 7: Apoptosis in E12.5 FL cells. E12.5 FL cells were stained with CD71 and Ter119 to analyze red cell differentiation, and then populations II (CD71+ Ter119-/low) and III (CD71+ Ter119+) were analyzed for apoptosis using Annexin V and DAPI staining. No significant difference was observed in early apoptosis (Annexin V+ DAPI-) or late apoptosis (Annexin V+ DAPI+) in the (A, B) II and (C, D) III populations in *Rpl5*+/- versus wildtype embryos. WT=6, *Rpl5*+/- n=6 (2 litters).

Supplemental figure 8: CBCs in adult and aged mice show no abnormality. CBCs were performed in young mice (7 weeks old, WT n=10, *Rpl5*+/- n=10; 5 female, 5 male in each group). No significant deviations from normal were observed in (A) hemoglobin (B) MCV (C) platelets (D) WBC (E) ANC (F) ALC for young mice. CBCs were performed in aged mice (WT n= 11, age range 5 – 22 months, *Rpl5*+/- n=7, age range 5 – 17 months). No abnormalities were seen in (G) hemoglobin (H) MCV (I) platelets, (J) WBC, (K) absolute neutrophil count (ANC) or (L) absolute lymphocyte count (ALC). The line represents the median value for each group.

Supplemental figure 9: Analysis of BM erythroid differentiation profiles in adult animals. Whole bone marrow was analyzed by flow cytometry for erythroid cell markers (Ter119, CD44) after exclusion of

nonerythroid cells (CD45+, Gr-1+, CD11b+, CD3+ and dead cells). (A) No significant difference in Ter119 mean fluorescent intensity or (B, C) in the % of the proerythroblast population ($Ter119^{low}CD44^{hi}$) was found between the BM of *Rpl5*+/- and WT adult mutant animals. WT n=3, *Rpl5*+/- n= 3, age 5 months.

Supplemental figure 10: Analysis of HSPC populations in the BM and spleen of adult animals. (A) Analysis of hematopoietic populations in WT and *Rpl5*+/- mice was performed by flow cytometry. WT n=5, *Rpl5*+/- n=5 (female mice, age 7-8 months). All counts were normalized by weight (A). No significant defects were seen in: (B) BM cellularity, (C) % LT-HSC (CD150+CD48-LSK), (D) % LSK, (E) % HPC1/2 (CD48+LSK), (F) % MPP (CD150-CD48-LSK), (G) BM myeloid % (CD11b+Gr1+), (H) BM T cell % (CD3+), (I) BM B cell % (B220+), (J) spleen cellularity, (K) spleen myeloid %, (L) spleen T cell % or (M) spleen B cell % populations.

Supplemental methods:

DNA extraction and genotyping

Genomic DNA was extracted from mouse tail or embryonic yolk sac using the EZ-10 Spin Column Animal DNA Mini-Preps kit (BS628, Bio Basic Inc. Canada, ON). Genotypes were confirmed for all mice included in the study. Genotyping was done by PCR using genomic DNA and the following primers: an exonic primer 5′ CGTGCTGGTGGTGCTACATA 3′ and intronic primer 5′ GGCCTCCACTGACAGACACT 3′. PCR amplification was done using Q5 High-Fidelity DNA Polymerase (NEB, cat# M0491L) as suggested by the manufacturer. PCR conditions consisted of 30 seconds (s) at 98°C followed by 35 cycles with each cycle consisting of 10s at 98°C, 15s at 67°C, 15s at 72°C, followed by one cycle of 2 min at 72°C. The PCR products were visualized on 1.2% agarose gels. Direct dye terminator sequencing of PCR products was done on an Applied Biosystem's 3730xl DNA Analyzer technology.

Genotyping by allele-specific PCR

We established an allele-specific PCR using 3 primers, which were designed using Primer1 software (http://primer1.soton.ac.uk/primer1.htm), in standard PCR reactions to specifically identify the *Rpl5* mutant “C” allele. Primers 2FO (forward outer) and 2RO (reverse outer) (5’ CAT CGC CCA TCC TCC ATG CTC

GTT GAG 3' and 5' CGG CAG CCA TTA GGC CAT GCT GGA AC 3', respectively) flank a "T" to "C" SNP mutation and amplified a 393 bp amplicon from *Rpl5* wild type and heterozygous genomic DNAs. Primer 2FI (forward inner) sequences (5' GGG TCT CTA TTC CGC AGG ATG GTG C**G**C 3') include the "C" allele SNP mismatch (in bold) and another deliberate mismatch at -2 position from the 3' terminus (underlined). Primers 2FI and 2RO generate a 192 bp amplicon that is specific to the "C" mutant allele. The specificity of these primers was verified using *Rpl5* genomic DNA samples that had been previously confirmed by Sanger sequencing.

Skeletal studies

Digital x-rays on adult mice were collected on a Faxitron Ultrafocus instrument. We performed whole-mount Alcian blue and Alizarin red staining of skeleton by euthanizing newborn (day 1-2) mice, removing skin and internal organs and fixing mice in 95% ethanol for 6 days. Samples were then stained overnight in 0.015% Alcian blue solution containing 80% ethanol and 20% acetic acid. Samples were then put back into fresh 95% ethanol for at least 3 hours before transferring into 2% KOH to remove remaining soft tissues. Skeletons were then stained with 0.005% alizarin sodium sulphate in 1% KOH for 12-14 h, then cleared in a solution of 1% KOH and 20% glycerol for at least 3 days and imaged using a dissection microscope (Nikon SMZ 745T). At least 4 newborn mice per group were analyzed for skeletal analysis and data presented as mean ± SD. Linear measurements of skulls and long bones were made using ImageJ software from NIH (version 1.52a). Two-tailed unpaired t-test with equal SD using Graphpad Prism 6.0 (Graphpad Software, Inc.) was used to identify the difference between the two genotypes. The difference was considered statistically significant when *p*-value was less than 0.05.

RT-qPCR

Spleen cells were isolated from WT and *Rpl5*+/- mice and lymphocytes were activated in culture with 10 µg/ml LPS for 48 hours. Total RNA was isolated using High Pure RNA Isolation kit (Roche). Reverse transcription was performed using iScript CDNA Synthesis kit (Bio-Rad) and quantitative real-time PCR performed using Power Sybr Green PCR Master Mix (Applied Biosystems/Thermo Fisher). Intron-spanning primers were designed using Primer3web version 4.1.0 (http://bioinfo.ut.ee/primer3/): Rpl5

forward GGCGAGAGGGTAAAACTGAC, Rpl5 reverse ATCCCCTTCTATACGGGCAT, beta actin forward GAGGCATACAGGGACAGCAC, beta actin reverse CTAAGGCCAACCGTGAAAAG. Relative mRNA expression was calculated using the ΔΔCt method and normalized to wildtype cells.

Blood analysis and flow cytometry

After euthanasia, blood was drawn by cardiac puncture in adult animals and placed into EDTA tubes. Blood counts were performed using Advia® 120 (Siemans) or VetScan® HM5 Hematology Analyzer (Abaxis). For newborn animals (P1-3), euthanasia was performed by decapitation and blood collected for blood cell counts. Blood samples of newborn animals were diluted 1:10 in PBS prior to analysis in order to obtain sufficient volume to measure. For analysis of hematopoietic stem and progenitor cells, we isolated adult bone marrow and livers of E12.5, E14.5 and P1-3 pups. Cells were incubated with CD16/CD32 Fc block then stained with antibodies in supplemental Table S1. Antibodies for HSPC, mature myeloid and lymphoid analysis are listed in supplemental Table S2. Events were quantified on a Fortessa flow cytometer. Data were analyzed using FlowJo software v. 9.7.6 (TreeStar, San Carlos, CA).

Cardiac and craniofacial studies

MicroCTs were performed using μCT100 (Scanco Medical, Bassersdorf, Switzerland) to assess craniofacial structures in adult mice. Three dimensional images were analyzed as outlined in using the MicroView image viewer (Parallax Innovations). For cardiac and craniofacial histology, the tissues were processed, sectioned, and stained by hematoxylin and eosin according to standard protocols. Images were photographed on a Leica DMI3000B microscope using an Olympus DP71 camera and DP controller and manager software.

Table S1: Antibodies/reagents used for western blot/erythroid studies

Antibody	**Source**	**Product number**	**Experiment**
mouse monoclonal anti-vinculin, clone hVIN-1	Sigma	V9131	Western blot 1:10,000
rabbit monoclonal anti-RPS19	Abcam	ab181365	Western blot 1:10,000
rabbit polyclonal anti-RPL5	Cell Signaling	14568	Western blot 1:1000
APC anti-mouse Ter119	Biolegend	116212	Flow cytometry E12.5, E14.5
FITC anti-mouse CD71	Biolegend	113806	Flow cytometry E12.5, E14.5
APC/Cy7 anti-mouse CD44	Biolegend	103028	Flow cytometry E12.5, E14.5
PE Annexin V	BD Biosciences	556421	Apoptosis flow cytometry E12.5
DAPI	Biolegend	422801	Flow cytometry E12.5, E14.5
LIVE/DEAD™ Fixable Aqua stain	ThermoFisher Scientific	L34957	Newborn flow cytometry
PE CD45	BD Biosciences	553081	Newborn flow cytometry
PE Gr-1	BD Biosciences	553128	Newborn flow cytometry
PE CD11b	BD Biosciences	557397	Newborn flow cytometry
PE CD3	BD Biosciences	555275	Newborn flow cytometry
FITC Ter119	BD Biosciences	561032	Newborn flow cytometry
APC CD44	BD Biosciences	559250	Newborn flow cytometry

Table S2: Antibodies used for flow cytometry studies of stem/progenitor, mature myeloid/lymphoid cells

Target	Fluorochromes	Clone	Source
CD150	PE-Cy7	TC15-12F12.2	Biolegend
CD48	AlexaFluor700	HM48-1	Biolegend
CD16/32	PE-Cy7	93	Biolegend
CD34	FITC	RAM34	eBiosciences
Sca-1	Percp-Cy5.5	D7	Biolegend
cKit	APC	2B8	Biolegend
Ter119	PE,FITC	TER-119	Biolegend
B220	PE,FITC	RA3-6B2	Biolegend
CD2	PE,FITC	RM2-5	Biolegend
CD3	PE,FITC	17A2	Biolegend
CD5	PE,FITC	53-7.3	Biolegend
CD8	PE,FITC	53-6.7	Biolegend
CD11b	APC	M1/70	Biolegend
Gr1	PE-Cy7, PE, FITC	RB6-8C5	Biolegend

Table S3: Partial alignment of *Rpl5* genomic sequences showing the ATG start codon followed by partial sequences of intron 1 The *Rpl5*c.3 +6T, indicated in red and by an arrow, is absolutely conserved across all 9 species analyzed.

Species	↓
mouse *Rpl5*	ATGgtgagtgggcatctgggtc
human *RPL5*	ATGgtgagtggatgcctcggtc
macaque *RPL5*	ATGgtgagtttatgcctcggtc
dog *RPL5*	ATGgtgagtggatatc-tggaa
rat *Rpl5*	ATGgtgagtgggcatctgggtc
chicken *Rpl5*	ATGgtcagtaccggcccgtacg
frog *Rpl5*	ATGgtcagtaaaccggagcaat
zebra *Rpl5a*	ATGgtcagtaaatctccaaaat
fly *Rpl5*	ATGgtaggtgctatagaaaagc

Accession numbers:
mouse *Rpl5*, ENSMUST00000082223.13; human *RPL5*, ENST00000370321.8; macaque *RPL5*, ENSMMUT00000007154.4; rat *Rpl5*, ENSRNOT00000030428.3; dog *RPL5*, ENSCAFT00000083197.1; chicken *Rpl5*, ENSGALT00000068972.2; frog *Rpl5*, ENSXETT00000049753.4; zebrafish *Rpl5a*, ENSDART00000005944.8; fly *Rpl5*, FBtr0344793.

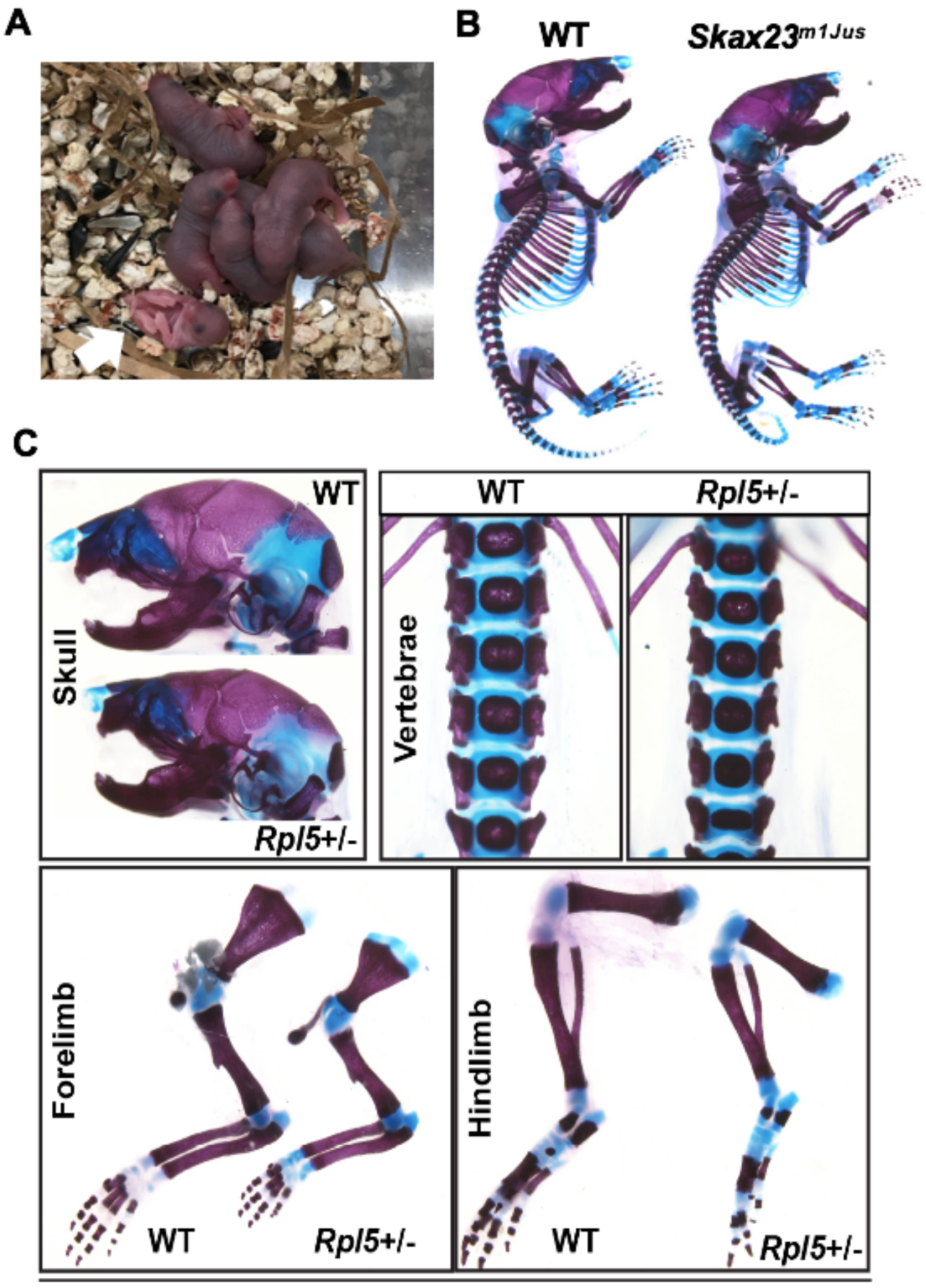

Supplemental figure 1

A

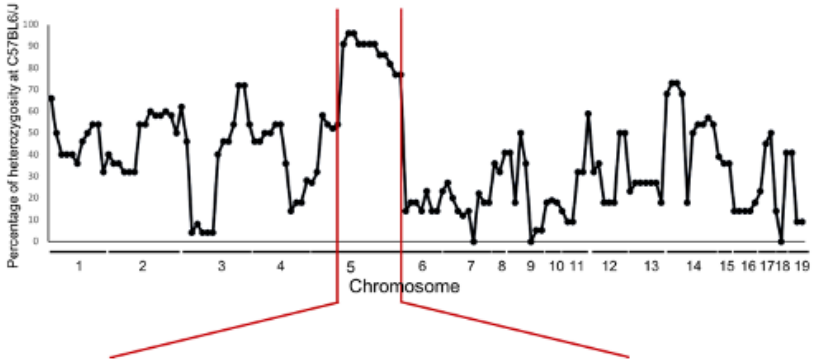

B

SNP	Position	129S6/SvEv	C57BL/6	Mice with kinky tail phenotype					
				N=11	N=6	N=1	N=1	N=1	N=1
rs13478433	104357881	TT	CC	CT	TT	TT	CT	TT	TT
rs13478451	109083680	CC	TT	CT	CT	CT	CT	CT	CT
rs32103915	112501418	AA	TT	AT	AT	AT	AT	AT	AT
rs29534493	115004548	TT	CC	CT	CT	CT	CT	CT	CT
rs13478483	118405516	TT	CC	CT	CT	CT	CT	CT	TT
rs8239888	122017784	CC	TT	CT	CT	CT	CT	CT	CC
rs3671202	125290118	CC	TT	CT	CT	CT	CT	CT	CC
rs13478518	128264874	CC	TT	CT	CT	CT	CT	CT	CC
rs13478539	133538654	TT	CC	CT	CT	CT	CT	TT	TT
rs13478542	135358216	CC	TT	CT	CT	CT	CT	CC	CC
rs29779884	141325735	TT	CC	CT	CT	CT	TT	TT	TT
rs13478574	144868252	CC	TT	CT	CT	CC	CC	CC	CC
rs3718776	150393126	TT	CC	CT	CT	TT	TT	TT	TT

C

SNP	Position in MB	129S6/SvEv	C57BL/6	Mice with kinky tail phenotype			
				N= 12	N=1	N=10	N=7
rs13478433	104.357881	TT	CC	CT	TT	TT	TT
rs29559613	106.480504	AA	GG	AG	AG	AA	AA
rs13478444	107.112543	AA	GG	AG	AG	AA	AA
rs4225396	108.071336	GG	AA	AG	AG	AG	AG
rs13478450	108.976897	CC	TT	CT	CT	CT	CT
rs13478451	109.083781	GG	AA	AG	AG	AG	AG
rs3665124	110.024336	AA	--	AG	--	AG	AG
rs3708939	111.010799	CC	TT	CT	CT	CT	CT
rs32071323	111.778516	AA	GG	AG	AG	AG	AG
rs32103915	112.501418	AA	TT	AT	AT	AT	AT
rs48981817	114.608657	GG	AA	AG	AG	AG	AG
rs29534493	115.004548	TT	CC	CT	CT	CT	CT
rs33727786	116.673508	AA	TT	AT	AT	AT	AT
rs3023051	117.668111	GG	AA	AG	AG	AG	AG
rs13478483	118.405516	TT	CC	CT	CT	CT	TT

Supplemental figure 2

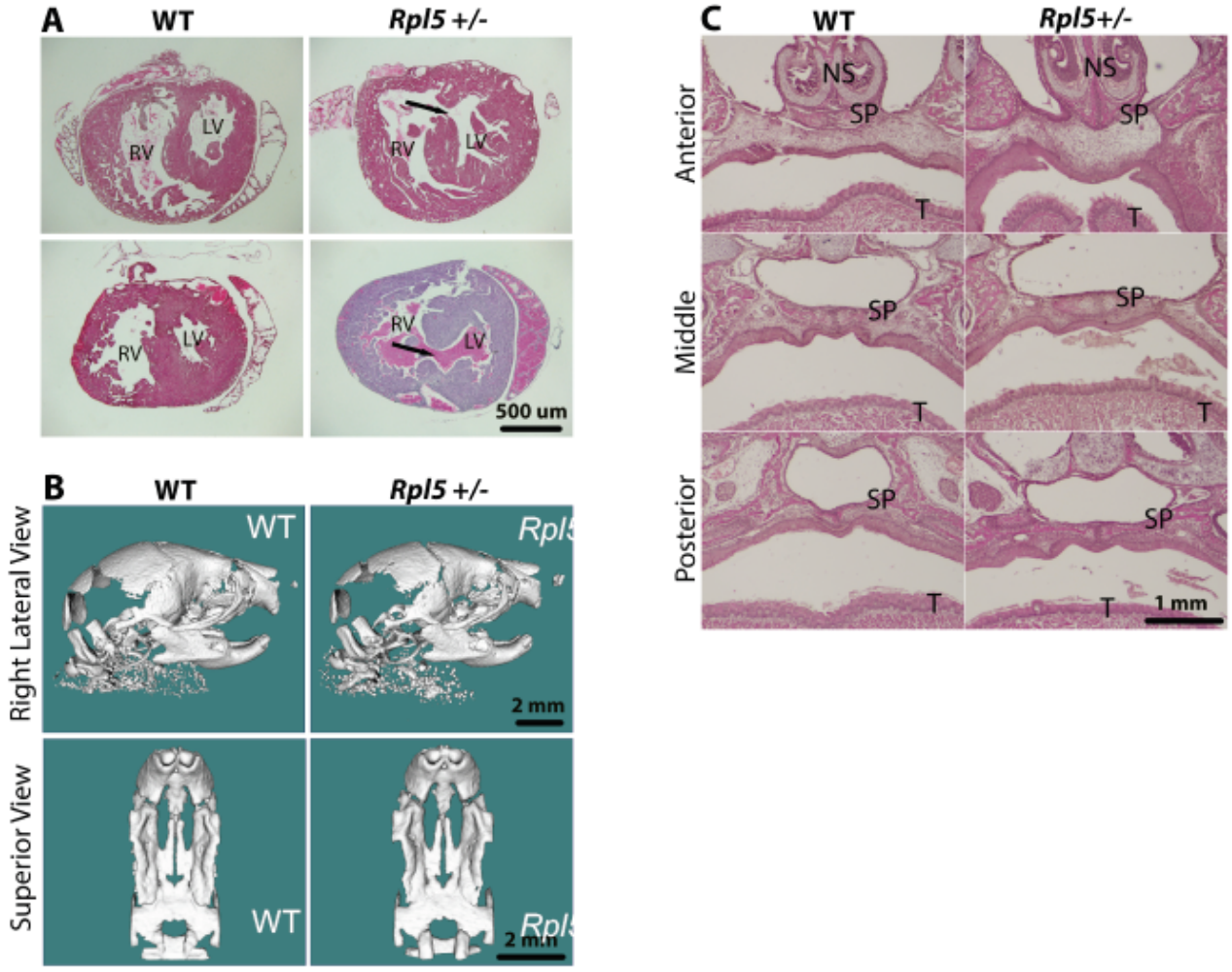

Supplemental figure 3

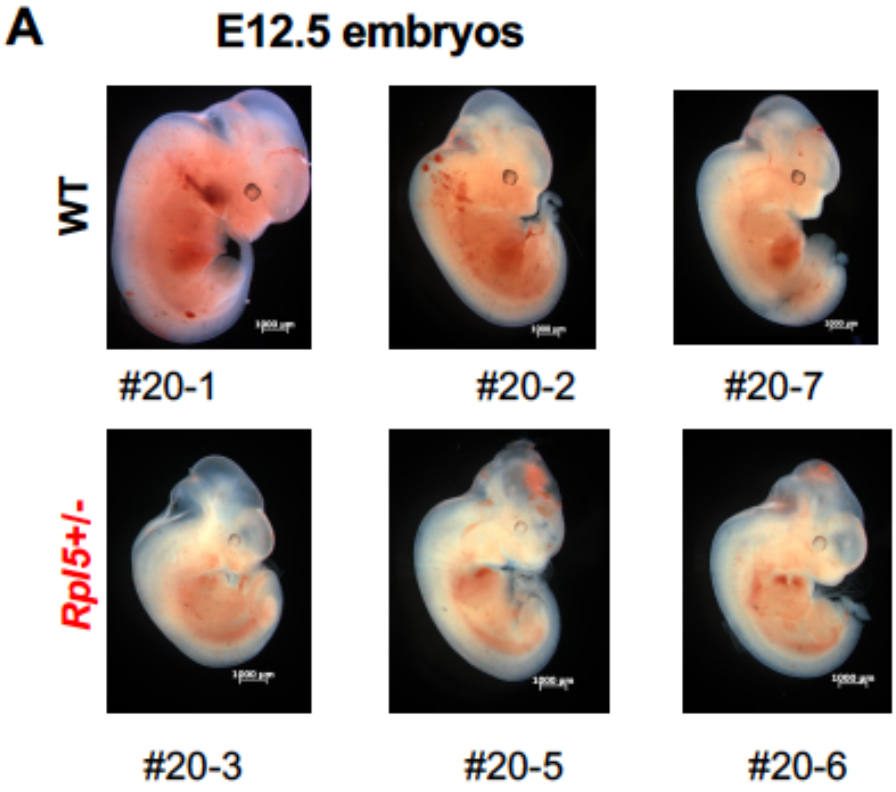

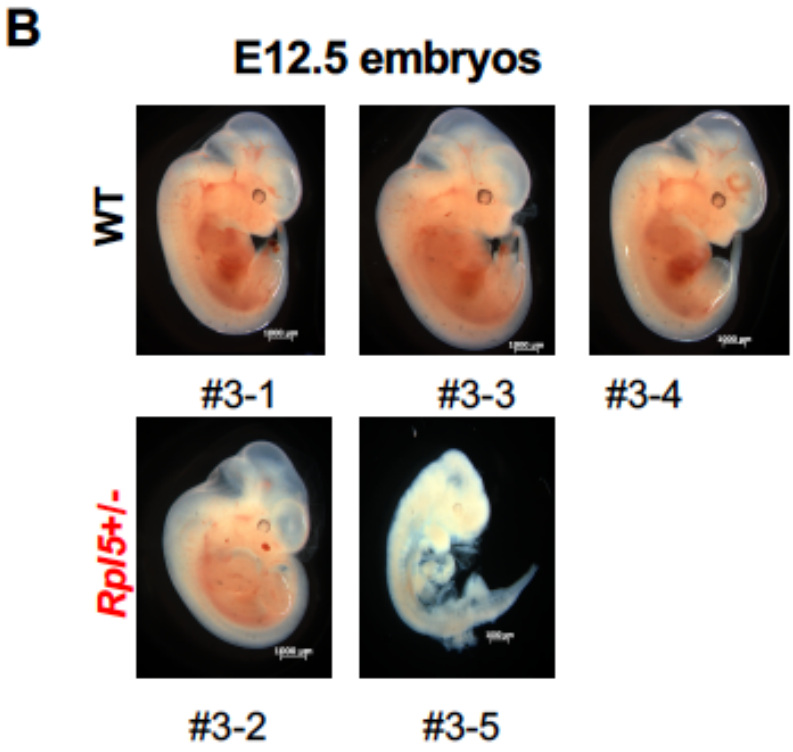

Supplemental figure 4

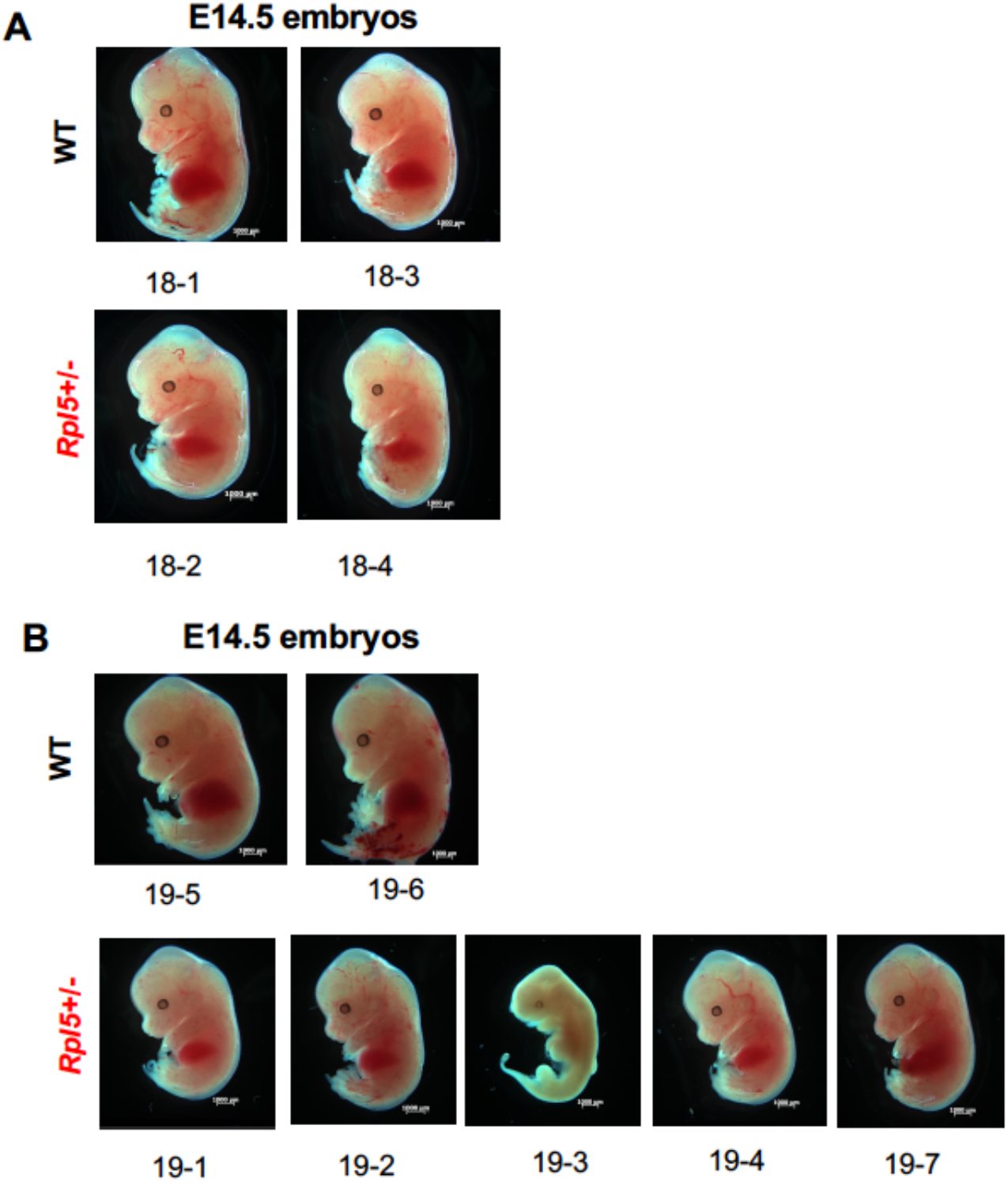

Supplemental figure 5

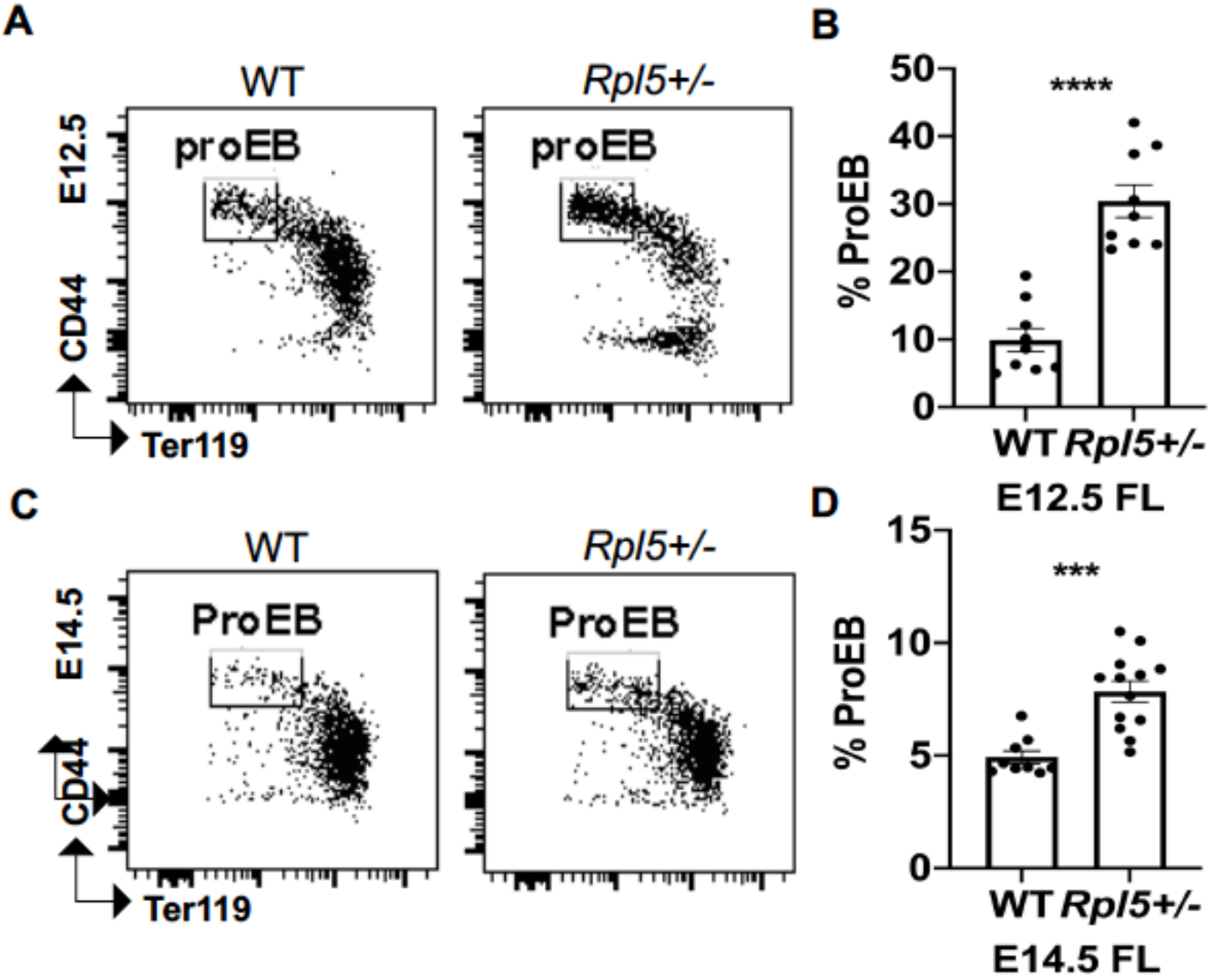

Supplemental figure 6

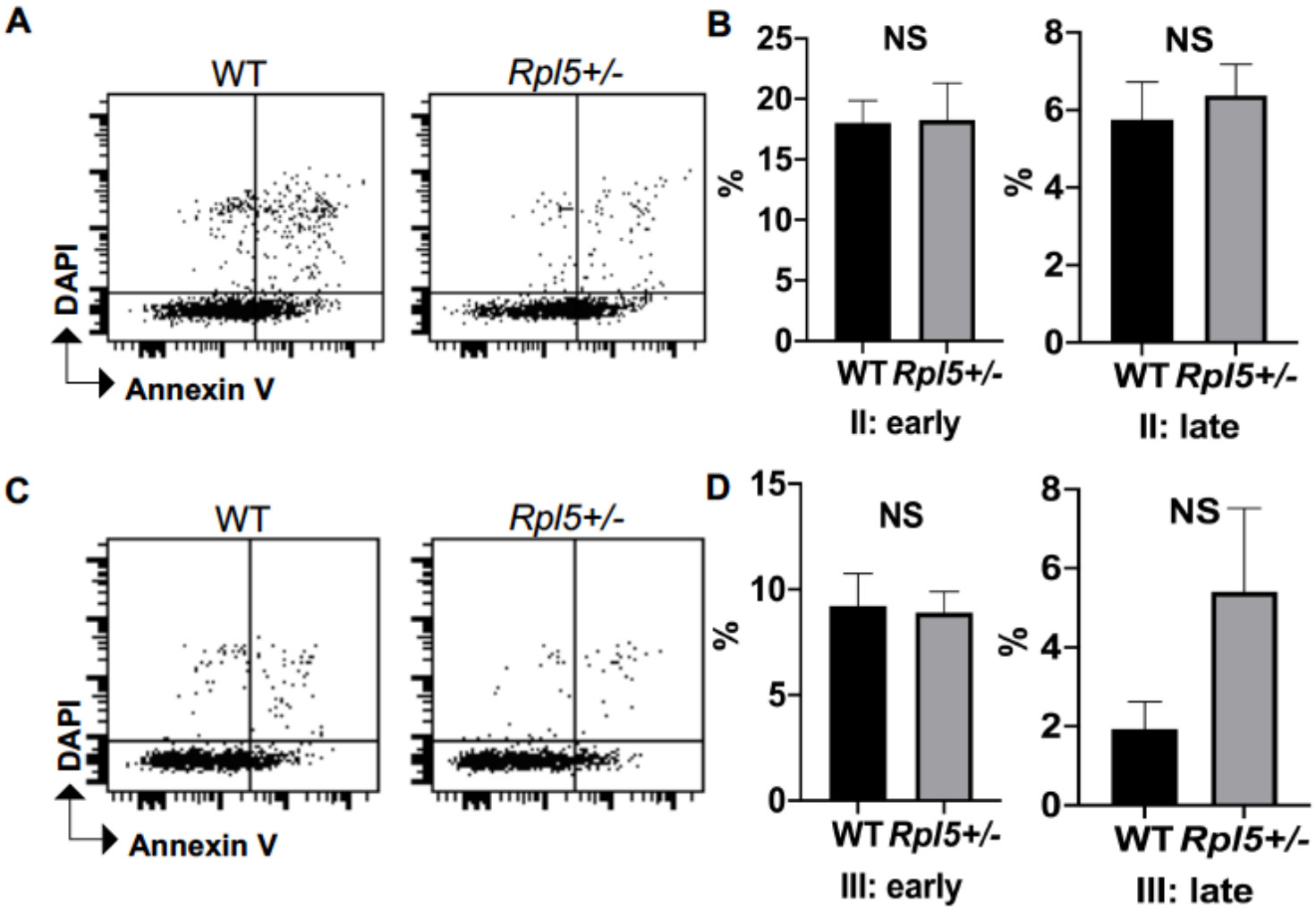

Supplemental figure 7

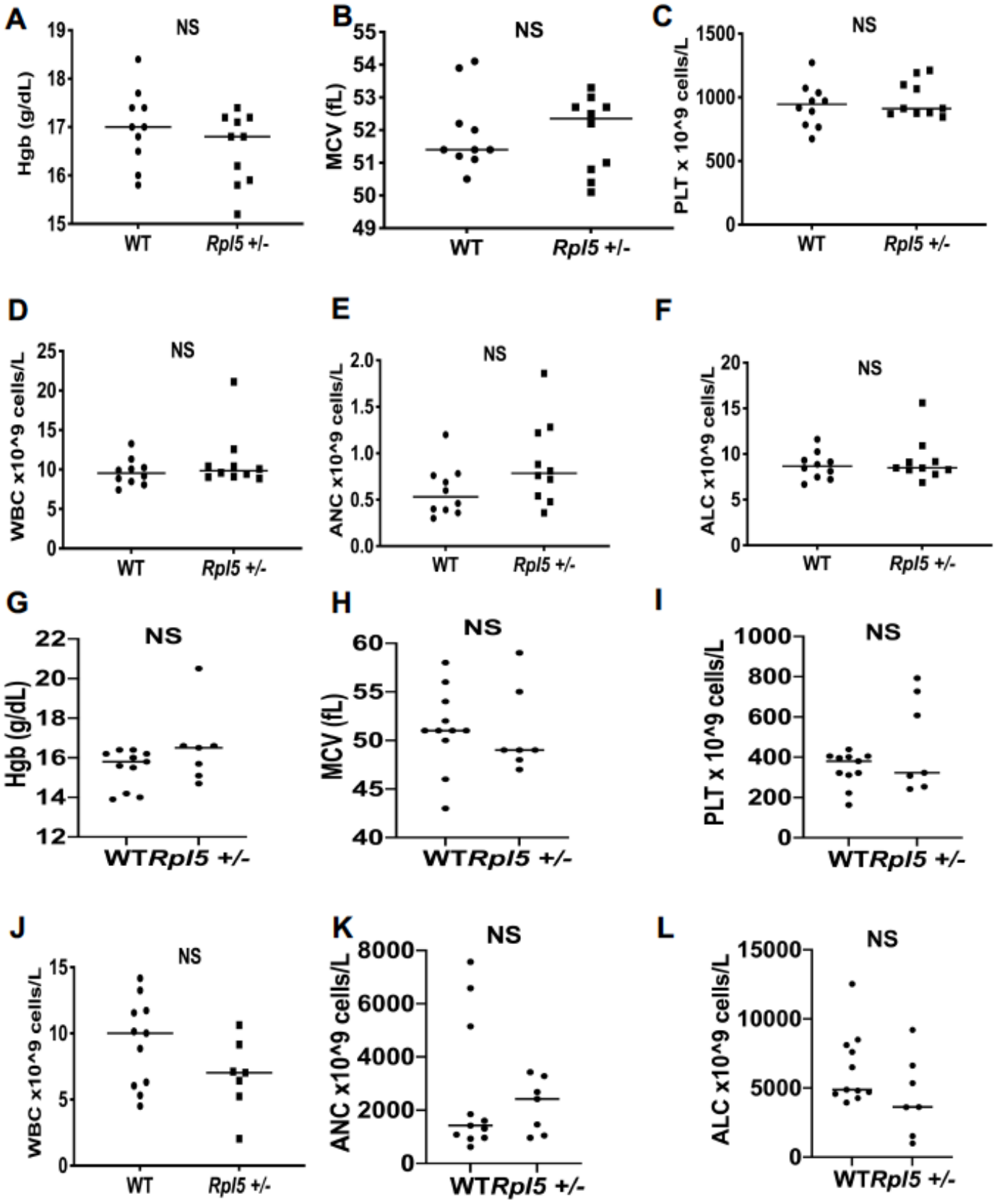

Supplemental figure 8

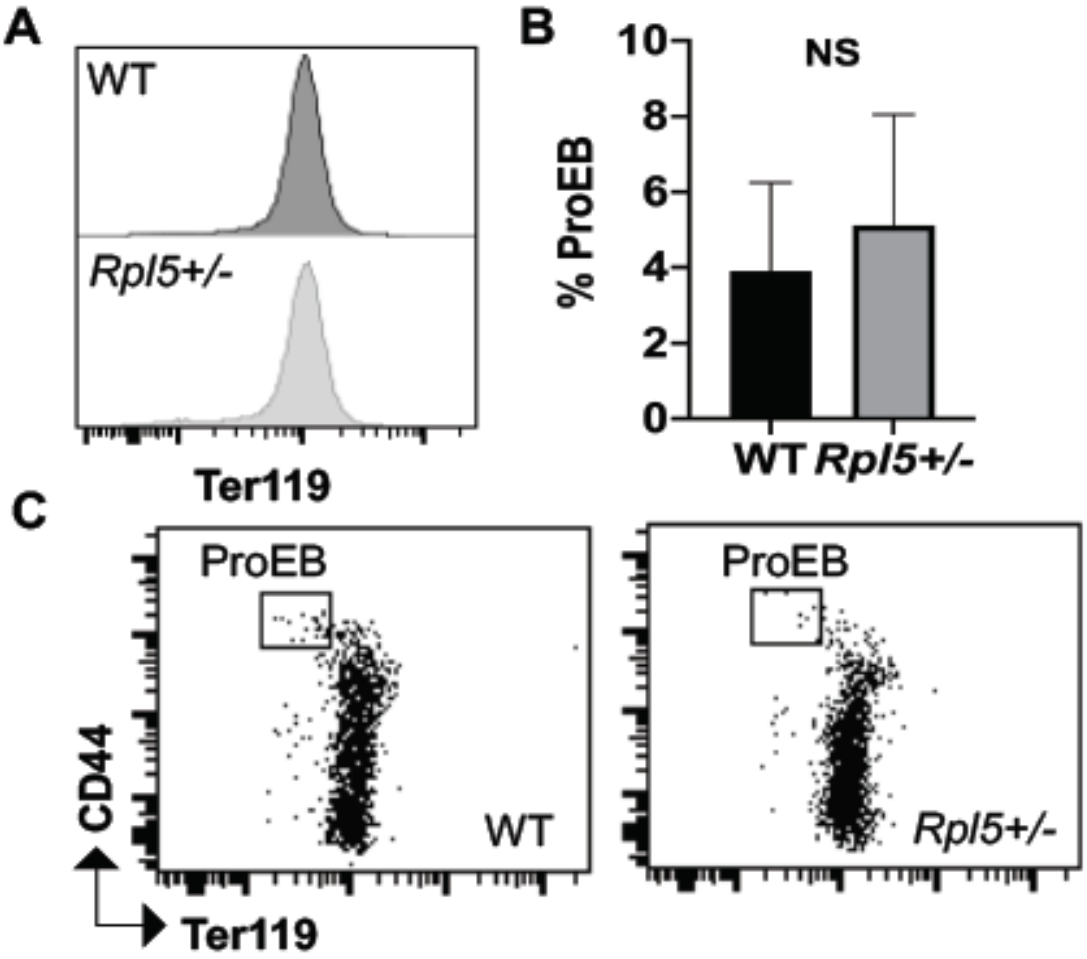

Supplemental figure 9

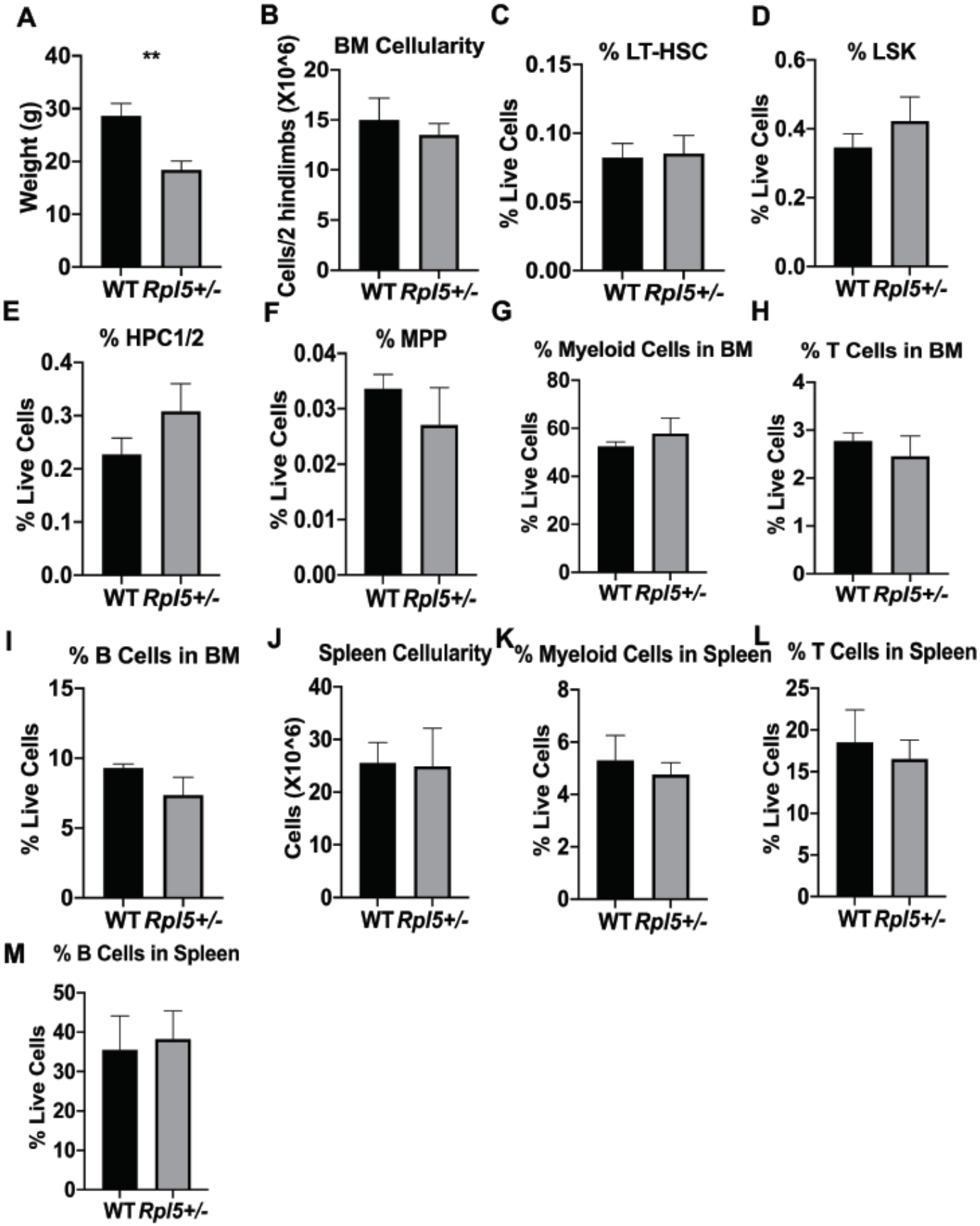

Supplemental figure 10